



## Original article

# Fabrication of multiwalled carbon nanotubes/carrageenan-chitosan@ Ce and Sr substituted hydroxyapatite biocomposite coating on titanium: *In vivo* bone formation evaluations

Meng Chen<sup>a</sup>, Haoxuan Zhang<sup>a,\*</sup>, Shiyong Shan<sup>a</sup>, Yuanyuan Li<sup>b</sup>, Xiaoguang Li<sup>a</sup>, Dayong Peng<sup>a,\*</sup>

<sup>a</sup> Department of Orthopedics, The First Affiliated Hospital of Shandong First Medical University, No.16766, Lixia District, Jingshi Road, Jinan, Shandong Province 250014, China

<sup>b</sup> Department of Pharmacy, The First Affiliated Hospital of Shandong First Medical University, Jinan, Shandong Province 250014, China

## ARTICLE INFO

## Article history:

Received 25 September 2019

Revised 22 October 2019

Accepted 4 November 2019

Available online 20 November 2019

## Keywords:

Carrageenan

Chitosan

Carbon nanotubes

Hydroxyapatite

Nanocomposite

Titanium

## ABSTRACT

Mineral substituted hydroxyapatite (MHAp) is one of the most significant bony mineral parts that have been broadly utilized as bony substitution matters as a result of its cytocompatible and bioactive properties. Though, the utilization of hydroxyapatite as bony inserts is confined because of its poor mechanical and fragile properties. To conquer this deformity and to produce appropriate bony embed substance; hydroxyapatite is joined with biocompatible macromoles (kappa-Carrageenan (KCG) and chitosan (CTS)). To improve the mechanical strength of the hydroxyapatite based biocomposite, functionalized multiwalled carbon nanotubes (FMWCNT) is joined to the biocomposite, which has for quite some time been considered for hard and delicate tissue implant because of its remarkable auxiliary and mechanical characteristic properties. It is outstanding that FMWCNT platform is the most-conspicuous substance for the hard tissues reproduction. We have developed a novel FMWCNT/KCG@MHAp nanocomposite on titanium (Ti) implant. The developed nanocomposite coatings implants were portrayed by different strategies (SEM, XRD, TEM). The outcomes show the arrangement and homogeneous conveyance of constituents in the nanocomposite coatings. Addition of FMWCNT and KCG into the MHAp nanocomposite altogether improves the attachment quality and flexible modulus of the scaffolds. Moreover, the reactions of mesenchymal stem cells (MSCs) culture onto the nanocomposite coating show that the suitability of cells was significantly high for FMWCNT and KCG consolidated MHAp than for MHAp. Animal model examinations demonstrate the nearness of delicate osteoblast and fibrous tissue development with no noteworthy provocative symptoms, which recommends that the Addition of FMWCNT and KCG encourage the great biochemical role of MHAp. For load-bearing applications, examine in different bony models is expected to substantiate the medical accessibility. In this manner, from the acquired outcomes, we propose that FMWCNT/KCG@MHAp nanocomposite can be considered as a prospective possibility for orthopedic applications.

© 2019 The Author(s). Published by Elsevier B.V. on behalf of King Saud University. This is an open access article under the CC BY-NC-ND license (<http://creativecommons.org/licenses/by-nc-nd/4.0/>).

## 1. Introduction

Hard tissues (teeth and bone) repair or recovery is a prevalent and testing medical issue in hard tissue surgery. These days, an

ever-increasing number of people are being tormented with hard tissues deformities. Autogenic and allergenic bony is normally used to manage bony deformities. Conversely, it's outstanding that an autogenic bone needs an optional medical procedure to secure benefactor bony from the patient's own body and allergenic bony bear's danger of diseases and invulnerable reactions (Subramanian et al., 2018; Behera et al., 2019). In this way, patient's needs have prodded the improvement of artificial hard tissue substance fabrication, transplantation, surgical remaking and the utilization of synthetic prostheses (Wang et al., 2016; Sahan et al., 2018).

Numerous polymers have been utilized to fabrication of scaffolds, however those of regular cause is frequently favored on the

\* Corresponding authors.

E-mail addresses: 2283@sdhospital.com.cn (H. Zhang), 1540@sdhospital.com.cn (D. Peng).

Peer review under responsibility of King Saud University.



grounds that, when contrasted with manufactured partners, they go along more effectively with the necessities of biodegradability, cytocompatibility and nonappearance of poisonous quality that are compulsory in any biomedical application (Gumargalieva et al., 1998). Chitosan (CTS) and Keppa-carrageenan (KCG) are two marine-determined biopolymers which have a place with the previously mentioned class and have exhibited in a past report the capacity to collect into nanoparticles (Grenha et al., 2010). CTS is a cationic polysaccharide and introduces well-archived great properties for medication conveyance, for example, low lethality, cytocompatibility, and biodegradability (Pella et al., 2018).

Carrageenan is a high molecular weight anionic liner heteropolysaccharide got from marine algae, Rhodophyceae. KCG has been utilized as biomaterials for a few applications, and their cytocompatibility has been generally demonstrated in the literature (Zamora-Sequeira et al., 2018). Actually, KCG increased much consideration due to their hydrophilicity, biocompatibility, and solid holding with enzymes and proteins. All the more significantly, KCG is basically like the glycosaminoglycans that are found normally in human hard tissue and ligament, and their capacity to help cell attachment and multiplication make them appropriate for scaffolding (Ocampo et al., 2019). Indeed, natural polymers, for example, cellulose, the most inexhaustible bio-polymer in nature, and its subordinates have already been utilized as a template to store minerals like HAp (Mao et al., 2018; Ogiwara et al., 2015). Therefore, cellulose has a prospective clinical application in orthopedic tissue engineering. Conversely, KCG offers points of interest over cellulose: in contrast to cellulose, the previous natural polymer is exceptionally solvent in aqua and expels the requirement for the substance or potentially physical change to its formation to acquire consistent composite.

Hydroxyapatite (HA), a fundamental inorganic segment of bone, is bioactive hydroxyapatite bioceramic that is utilized in surgery to supplant and imitate bone. Whereas hydroxyapatite biologically active implies it has a noteworthy capacity to advance bone development along its exterior, its mechanical properties are lacking for significant load-bearing gadgets. To tackle this issue, strengthening phases are typically brought into biocomposites (Singh et al., 2008).

A perfect strengthen substance would grant mechanical integrity to the biocomposite at low loadings, without lessening its biocompatibility (White et al., 2007). Owing to their little measurements, high perspective proportion, and high quality and rigidity, MWNT has stirred a few analysts' enthusiasm for the biomedical territory (Bounioux et al., 2012; Chatterjee et al., 2016). Particularly, HAp and MWNT are frequently applied in biocomposite substances to improve their mechanical properties and biocompatibility (Zhu et al., 2011).

Electron beam treatment (EBT) is novel routes for the alteration of embed surfaces to deliver a high level of immaculateness with enough irregularity for superior osseointegration (Surmeneva et al., 2015). EBT can bring about novel microstructures with expanded roughness, helpful surface properties of metallic implants. Besides, ongoing investigation demonstrated that EBT is another strategy for treating insert exteriors to deliver a high level of immaculateness with improved consumption osseointegration (Chinh et al., 2019). Combination of the EBT and the deposition of biocomposite onto the outside of titanium can open up new open doors for the biodegradable biocomposite advancement with the improved mechanical characteristics.

In this paper, the development and portrayal of a nanocomposite (FMWCNT/KCG-CTS/MHAp), is accounted for. The mix of FMWCNT and KCG-CTS with MHAp gave off an impression of being a sensible methodology for mirroring regular bone, as this brought about a striking improvement of their mechanical characteristic and cytocompatibility. Consequently, the fabricated nanocompos-

ite scaffold will be conceivably appropriate for bone tissue engineering applications.

## 2. Materials and methods

### 2.1. Implant coating preparation

The states of the PEB treatment (PEB producer "SOLO") were as per the following: electron shaft vitality thickness: 15 J/cm<sup>2</sup>, electron pillar beat term: 50 μs. A normal electron vitality in the shaft was 16 keV. The functionalization of MWCNT was completed as per past work (Chinh et al., 2019). Additionally, CTS-KCG nanoparticles were set up by a recently portrayed technique (Mohamadnia et al., 2008). The electrochemical testimony of MHAp (calcium + strontium + zinc) to phosphate proportion of 1.67, and nanocomposite was performed in a three-electrode framework where the Pt terminal was utilized as a counter anode and with SCE and titanium as a source of perspective and working cathode, individually. The MHAp, and nanocomposite was electrodeposited on titanium at -1.4 V versus saturated calomel electrode utilizing the electrochemical workstation. After the electrodeposition procedure, the coated implants were delicately washed with deionized aqua and afterward dried at RT for one day.

### 2.2. Surface characterization

The recognizable proof of the crystalline phase of the specimen was inspected by XRD (D8 advance, bruker-axs). The sub-atomic structure was portrayed by Fourier change infrared spectrometry (FTIR, Alpha, Bruker, USA). Transmission electron microscopy (TEM) investigations of tests arranged on carbon covered 200 mesh Cu lattices were performed utilizing JEOL JEM-2100. The covering microstructure was surveyed by SEM (Camscan MaXim2040S) at 15 kV in backscattering mode; while the covering semi-quantitative microanalysis was resolved utilizing EDS (Quantax XFlash 6130, Bruker).

### 2.3. Adhesion strength analysis

The adhesion strength of the MHAp and nanocomposite coatings on titanium embed was done by the destroy out the test as indicated by the ASTM worldwide standard F1044-05, with triple analyses for each specimen. The specimens were exposed to tests at a consistent cross-head speed utilizing an all-inclusive testing machine.

### 2.4. Protein adsorption mesenchymal stem cells on prepared implants

Protein adsorption was estimated by a past report (Zhuo et al., 2012). Cell culture medium comprised of Dulbecco's modified Eagle's medium-low glucose enhanced with ten percent fetal bovine serum and one percent penicillin/streptomycin anti-infection agents. Stem cells were refined in a hatchery at RT with five percent carbon dioxide, and the culture was changed like clockwork. Cultures of ninety percent cells were trypsinized, washed and suspended in the crisp medium. Stem cells were seeded onto prepared implants. The reaction of stem cells was assessed by deciding cell multiplication, ALP and osteogenic qualities articulation of the mesenchymal stem cells.

### 2.5. Cell differentiation

Mesenchymal stem cells were seeded on prepared implants in osteogenic medium enhanced with penicillin/streptomycin. After culture for 6 and 12 days, the separation of cells was examined.

Complete cell RNA was separated from stem cells by Trizol. Here the gene articulation levels of bone OCN, collagen I and ALP were resolved after the techniques portrayed beforehand (Li et al., 2004).

## 2.6. Animal model

Eighteen male New Zealand hares gauging a normal of 6 lbs were acquired from an authorized merchant. All animal studies were performed following institutional guidelines and approved by the Institutional Animal Care and Use Committee. The hares were anesthetized employing an intravenous infusion of xylazine and ketamine hydrochloride and were set in the recumbent location. A straight cut was made in the territory of the hare's femur. Shallow sash and periosteal layer were chiseled utilizing a sharp analyzation to uncover bony surface. A bicortical opening of 0.002 m in distance across was made in both femur of the bunny utilizing a hardened steel drill of 0.002 m breadth. The specimen bars (distance across 0.002 m, stature 0.01 m) were situated utilizing finger weight and tenderly took advantage of the space of the opening, trailed by shutting the skin with nylon suture. Sums of thirty-six inserts, with twelve examples in each gathering, were haphazardly embedded into the hare's femurs. 9 hares were relinquished after the implantation of about a month and the other 9 hares following two months.

## 2.7. Statistical analysis

All of the experimental groups of the study were carried out in triplicate, and the results were analyzed using ANOVA statistical study.

## 3. Results and discussion

### 3.1. Chemical and phase analysis

FTIR spectra for the CTS-KCG, MHAp, and FMWCNT/CTS-KCG@MHAp nanocomposite are shown in Fig. 1A. The amide groups are veiled by the  $1636\text{ cm}^{-1}$  bowing band of adsorbed aqua and the  $1545\text{ cm}^{-1}$  absorption of the amino gatherings in protonated CTS (Kumari et al., 2016). For the MHAp and the FMWCNT/CTS-KCG@MHAp nanocomposite, the groups at  $588$ ,  $609$ ,  $945$ ,  $1023$ ,  $1087\text{ cm}^{-1}$  related to various vibration methods of the phosphate group in apatite, while the groups at  $646$  and  $3556\text{ cm}^{-1}$  symbolized to hydroxyl group as extending and

twisting vibration (Reyes-Gasga et al., 2013). On account nanocomposite, the major characteristic bands of FMWCNTs and CTS-KCG exist together and no new bands show up, reflected by the nearness of the crest at  $1710\text{ cm}^{-1}$  related with FMWCNTs and the tops at  $1622\text{ cm}^{-1}$  identified with CTS-KCG. This affirms electrostatic adsorption may happen between the protonated amine gatherings of CTS and the carboxylate bunches on the FMWCNTs, which encourages FMWCNTs to scatter in the CTS-KCG consistently.

Fig. 1B shows the XRD results of the nanocomposite. The planes positions are coordinating intently the diffraction planes of stoichiometric apatite (JCPDS card No. 9-0432) (Hasan et al., 2018). It is apparent that three extraordinary planes of precious phase stages at  $(0\ 0\ 2)$ ,  $(2\ 1\ 1)$  and  $(3\ 1\ 0)$  which are doled out to 25, 32 and 39 of crystalline apatite, separately. The spectra of the nanocomposite demonstrated expansive tops with poor crystallinity around the major diffraction area close to  $32$  ( $2\theta$ ), which recommended low crystallinity of apatite in the nanocomposite. This crystallographic phase of the nanocomposite was progressively like characteristic bone mineral (natural hydroxyapatite) (Chen et al., 2013). In this way, the apatite nanocrystallites in the nanocomposite have more similitudes with characteristic bone mineral as far as the level of crystallinity. Nonetheless, no FMWCNTs planes were found in the spectra, which may result from that the trademark planes of FMWCNTs and the diffraction planes of apatite is correspondent and the intensity of apatite diffraction planes is so solid.

### 3.2. Morphology analysis

Fig. 2 demonstrates the morphology of MHAp, and nanocomposite coated titanium. Fig. 2a demonstrates the pure FMWCNTs agglomerated uniform packed nanowire arrangement of the microstructure is demonstrated to give a further all the more comprehension of the FMWCNTs morphology, TEM pictures obviously appear in functionalization of MWCNTs as appeared in Fig. 2b. As well as the SAED image demonstrated in Fig. 2b (insert) the rings relating to FMWCNTs. The morphology of MHAp and nanocomposite coating onto titanium substrate treated with EBT was smoother on the micro and nanoscale level. Also, it tends to be seen that the coating on the treated surface-displayed homogenous granule structure features. TEM and SEM pictures great understanding for nanocomposite coating. Fig. 2B demonstrates the EDAX examination result shows the nearness of P, Sr, Ce and Ca element in the nanocomposite.

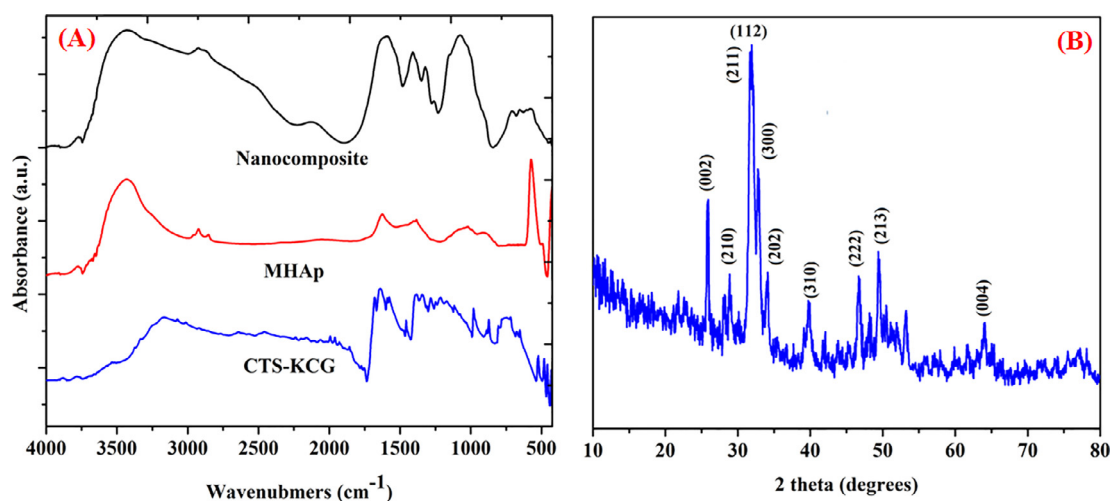
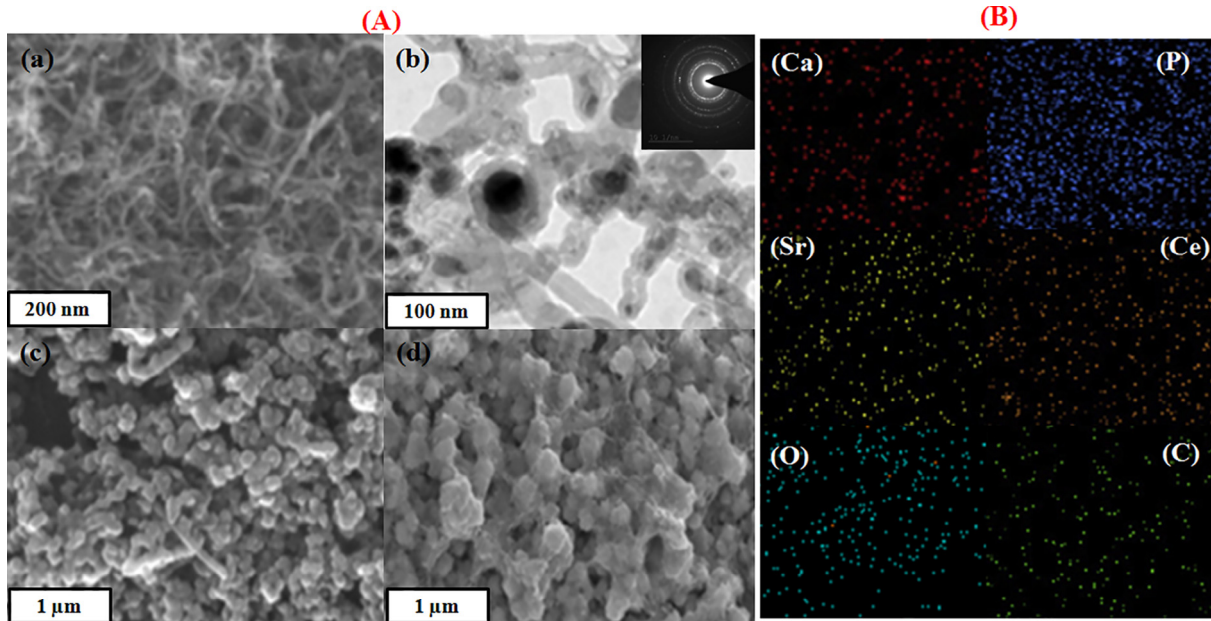


Fig. 1. (A) FTIR spectra of prepared samples, (B) XRD pattern of the nanocomposite.



**Fig. 2.** (A) SEM image of the f-MWCNT (a), TEM image of f-MWCNTs (b); SAED pattern of f-MWCNTs (b insert), SEM images of MHAp (d), nanocomposite (e). (B) Elemental mapping of nanocomposite.

### 3.3. Adhesion strength analysis

Micro-structural changes inevitably bring about a change in mechanical properties (Behnagh et al., 2012). To decide changes in mechanical properties with EBT and FMWCNT strengthen of MHAp, the haul out tests are performed and the outcomes are talked about underneath. The adhesion strength of the nanocomposite coating substrate is one of the hugest properties for the animal implantation. The adhesion strength of the MHAp and nanocomposite coatings individually was assessed and is appeared in Fig. 3. The bond quality for the MHAp was about 21 MPa, comparably, the nanocomposite coating indicated attachment quality of 29 MPa. Therefore, it is reasoned that the EBT and FMWCNT strengthen of MHAp has improved the bond strength between the resultant nanocomposite covering and titanium implant.

### 3.4. Protein adsorption

Fig. 4a demonstrates the aggregate sum of protein adsorbed on the substrates of pristine titanium, MHAp, and nanocomposite

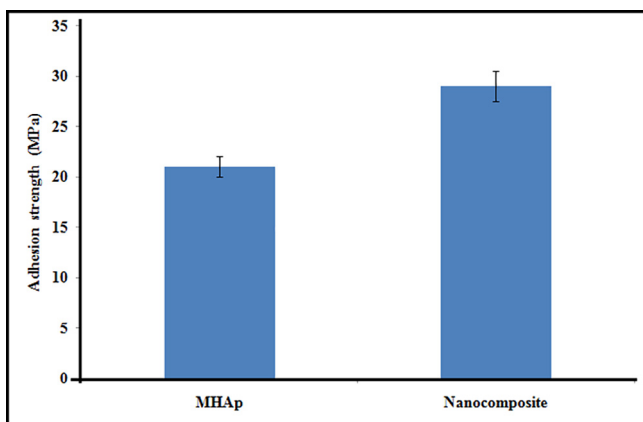


**Fig. 3.** Adhesion strength of MHAp and nanocomposite coatings on electron beam treated titanium.

coated implants. The measure of protein adsorbed on the nanocomposite surface was higher than that on MHAp, and was fundamentally higher than that on the titanium substrates. The nanocomposite surface consumed a lot of proteins, improved cell connection, expansion and osteogenic separation of stem cells, which thusly brought about upgraded bone recuperating in vivo. It is realized that osteogenic acceptance of cells around inserts in vivo is a significant factor in the useful rebuilding of the tissue.

### 3.5. In vitro cytotoxicity

The biocompatibility examine determines the stem cells feasibility on the composite, control, MHAp, nanocomposite which was refined for 1, 4, and 7 days. The cell feasibility of the coatings was determined the resultant rate has appeared in the bar graph in Fig. 4b. The rates of stem cell feasibility increments as the hatching days build which can be seen in fluorescence pictures found in Fig. 5. The nanocomposite demonstrated critical cell reasonability which is like that of the other materials. Nanocomposite group at day 1, the stem cells disseminated reliably and spread on the nanocomposite specimen. On day 4, the stem cells showed signs of improvement on the surfaces when contrasted with that on day 1. No dead cell can be seen from the specimen. As the brooding was improved to 4 days, the number of cells likewise expanded step by step. These are appointed that the nanocomposite has almost no toxicity and unquestionably bolster cell expansion. The nanocomposite at 7 days of culture demonstrated the presence of increasingly suitable cells which demonstrates that the biocompatible idea of the composite which isn't influenced by the nearness of mineral particles Sr and Ce in the composite. It is additionally evident that FMWCNT didn't influence the cell multiplication of the nanocomposite. Along these lines, the MTT examine test unmistakably demonstrated that the nanocomposite broadly improved by the suitability of cells which is the necessity for biomedical applications. These relative outcomes proposed that nanocomposite would be a cultivated looking for a composite to be utilized as a bone transplant for bone tissue engineering applications.

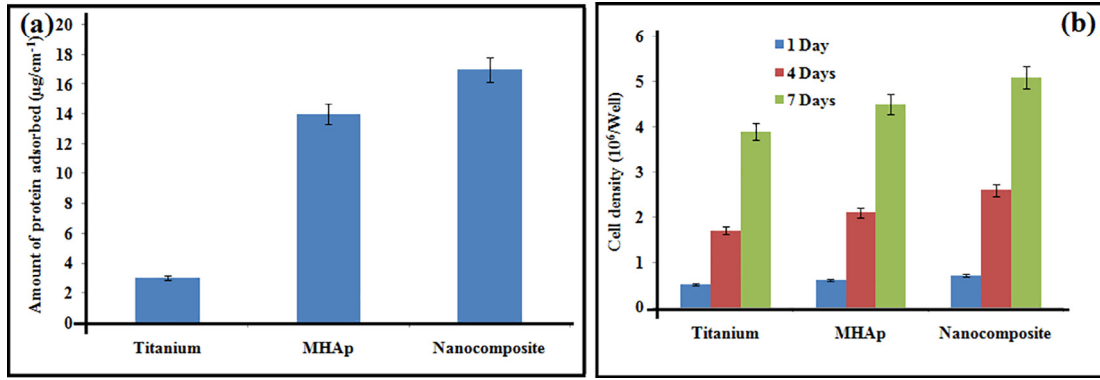


Fig. 4. Protein adsorption assay (a); proliferation on prepared samples.

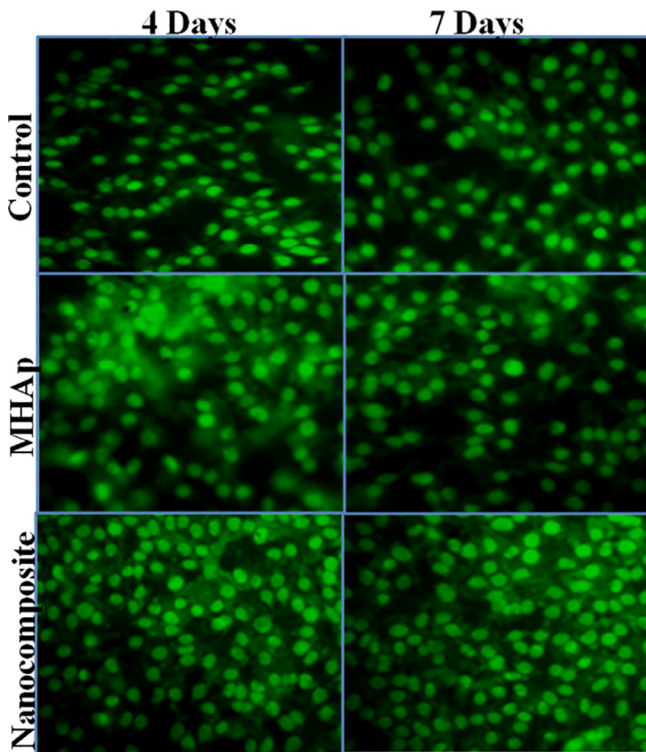


Fig. 5. Fluorescent microscopic images showing the stem cells on prepared samples at days of incubation (Scale bar = 50 µm).

### 3.6. Cell differentiation

Fig. 6a demonstrates the alkaline phosphatase activity expressed via stem cells on the MHAp and nanocomposite in the wake of refined for 6 and 12 days. The phosphatase activity of stem cells on the nanocomposite coated implant in the osteogenic medium was marginally higher than that on the MHAp implant and was essentially higher than that on the pristine titanium implant both at 6 and 12 days. Additionally, the articulation levels of alkaline phosphatase activity, collagen I and osteocalcin of MSCs on the MHAp and nanocomposite were comparative and essentially higher than those on pristine titanium implant at 12 days after incubation (Fig. 6b).

### 3.7. Histomorphological observation

The histological outcomes demonstrated that the interface of bony imperfections in the gathering of pristine titanium (control) was customary at one and two months (Fig. 7) the hard contact among bony and embeds were free so the bone was not hauled out alongside the inserts. The interfaces on MHAp appear to be more irregular than that on the pristine titanium bunch at both time focuses, which suggested the more grounded bone contact among bony and embeds so some bony was hauled out alongside the inserts. In the gathering of nanocomposite, some bony tissues were detached by hauling out the inserts and the enormous voids left, which implied that the bony was all the more firmly in contact with the nanocomposite embeds so some bone tissue was broken and stayed on the outside of inserts. The MT staining examination showed that general bony tissue canvassed the imperfections in

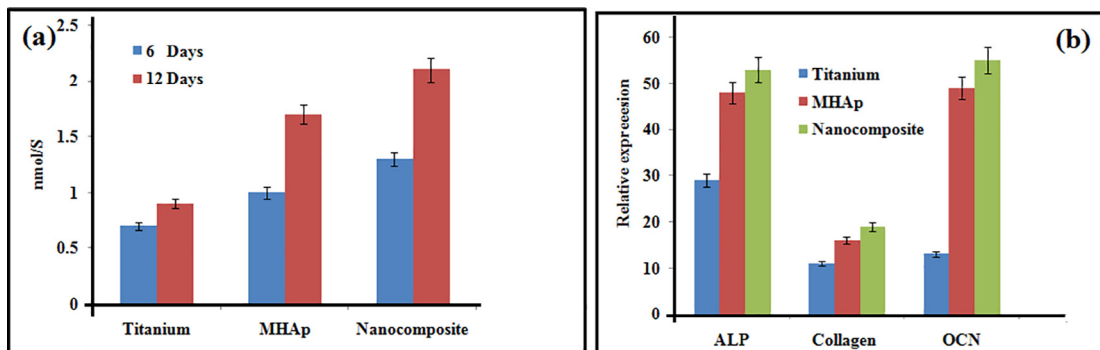


Fig. 6. ALP activity (a); and gene expression (b) on prepared samples.

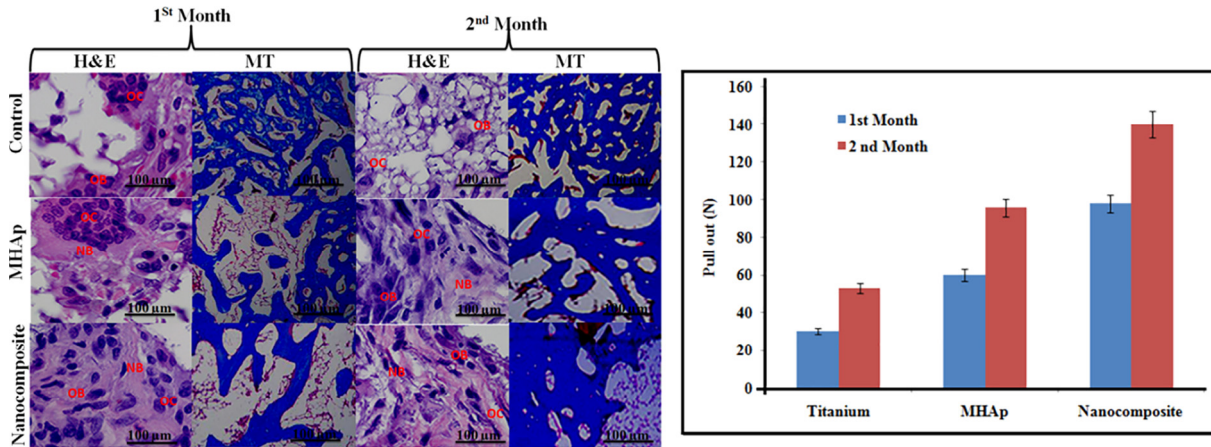


Fig. 7. (A) Bone defects for the implantation. (B) Pull-out value of implants at one and two month healing period.

the composite gathering, while probably some mineralized bony tissue was available in the MHAp and nanocomposite group at about a month. At about two months, a significant part of the mineralized bony tissue on the deformity site was noticeable in the nanocomposite gathering, yet this sum was much lower in the MHAp group.

### 3.8. Biomechanical test

Consequences of the mechanical test were communicated as the most extreme pull-out power in Fig. 7B, which we're reliably higher for the nanocomposite substrate than for the pristine titanium and MHAp implant substrate at one and two months of the recuperating time frame. The nanocomposite gathering applied the most grounded consequences for improving estimations of the three gatherings at both times focuses. The maximal haul out test power expanded by 1.5 and 0.5 creases contrasted with the pristine titanium and MHAp implant at about a month, and by 1.8 and 0.6 overlays at about two months, individually. The estimations of the MHAp implant likewise essentially expanded contrasted and the pristine titanium bunch at both times focuses, yet not more than the nanocomposite group.

## 4. Conclusion

This investigation plans to present a new nanocomposite as potential implants for bone tissue engineering applications. The physicochemical analysis affirms the presence of nanocomposite coating on titanium. For the clinical applications, the inserts need to fulfill various practical necessities, for example, biocompatibility and mechanical properties. Among the coatings implants, the nanocomposite coated implants is biocompatible with an improved cell expansion rate, interestingly with the majority of different coatings. The achievement of the fabricated coatings implants in bone tissue applications requires a decent comprehension of the bone-to-implant relationship with the association regarding the particular tissue recovery. This could be clear from the animal model investigation. Further, look into on nanocomposite in huge animals is required to assess their forthcoming use as orthopedic substitution materials.

### Declaration of Competing Interest

The authors declare that they have no known competing financial interests or personal relationships that could have appeared to influence the work reported in this paper.

## Acknowledgments

Authors grateful for the financial supports from the National Science Foundation for Young Scientists of China (Grant No.81902188).

## References

- Behnagh, R.A., Besharati Givi, M.K., Akbari, M., 2012. Mechanical properties, corrosion resistance, and microstructural changes during friction stir processing of 5083 aluminium rolled plates. *Mater. Manuf. Processes* 27, 636–640.
- Behera, D.R., Nayak, P., Rautray, T.R., 2019. Phosphatidylethanolamine impregnated Zn-HA coated on titanium for enhanced bone growth with antibacterial properties. *J. King Saud Uni.-Sci.*
- Bounioux, C., Katz, E.A., Yerushalmi-Rozen, R., 2012. Conjugated polymers-carbon nanotubes-based functional materials for organic photovoltaics: a critical review. *Polym. Adv. Technol.* 23, 1129–1140.
- Chatterjee, N., Yang, J., Kim, S., Joo, S.W., Choi, J., 2016. Diameter size and aspect ratio as critical determinants of uptake, stress response, global metabolomics and epigenetic alterations in multi-wall carbon nanotubes. *Carbon* 108, 529–540.
- Chinh, V.D., Speranza, G., Migliaresi, C., Van Chuc, N., Tan, V.M., Phuong, N.T., 2019. Synthesis of gold nanoparticles decorated with multiwalled carbon nanotubes (Au-MWCNTs) via cysteaminium chloride functionalization. *Sci. Rep.* 9, 5667.
- Chen, L., Hu, J., Shen, X., Tong, H., 2013. Synthesis and characterization of chitosan-multiwalled carbon nanotubes/hydroxyapatite nanocomposites for bone tissue engineering. *J. Mater. Sci. - Mater. Med.* 24, 1843–1851.
- Gumargalieva, K.Z., Horak, D., Zaikov, G.E., 1998. Biodegradable polymeric microparticles in biomedical applications. *Int. J. Polym. Mater.* 42, 83–117.
- Grenha, A., Gomes, M.E., Rodrigues, M., Santo, V.E., Mano, J.F., Neves, N.M., Reis, R.L., 2010. Development of new chitosan/carrageenan nanoparticles for drug delivery applications. *J. Biomed. Mater. Res. Part A* 92, 1265–1272.
- Hasan, M.M., Khan, M.N., Haque, P., Rahman, M.M., 2018. Novel alginate-dialdehyde cross-linked gelatin/nano-hydroxyapatite bioscaffolds for soft tissue regeneration. *Int. J. Biol. Macromol.* 117, 1110–1117.
- Kumari, S., Rath, P., Kumar, A.S.H., 2016. Chitosan from shrimp shell (Crangon crangon) and fish scales (Labeorohita): extraction and characterization. *Suneeta. Afr. J. Biotechnol.* 15, 1258–1268.
- Li, L.H., Kong, Y.M., Kim, H.W., Kim, Y.W., Kim, H.E., Heo, S.J., Koak, J.Y., 2004. Improved biological performance of Ti implants due to surface modification by micro-arc oxidation. *Biomaterials* 25, 2867–2875.
- Mao, D., Li, Q., Bai, N., Dong, H., Li, D., 2018. Porous stable poly (lactic acid)/ethyl cellulose/hydroxyapatite composite scaffolds prepared by a combined method for bone regeneration. *Carbohydr. Polym.* 180, 104–111.
- Mohamadnia, Z., Zohuriaan-Mehr, M.J., Kabiri, K., Jamshidi, A., Mobedi, H., 2008. Ionically cross-linked carrageenan-alginate hydrogel beads. *J. Biomater. Sci. Polym. Ed.* 19, 47–59.
- Ocampo, J.I.G., de Paula, M.M.M., Bassous, N.J., Lobo, A.O., Orozco, C.P.O., Webster, T. J., 2019. Osteoblast responses to injectable bone substitutes of kappa-carrageenan and nano hydroxyapatite. *Acta Biomater.* 83, 425–434.
- Ogiwara, T., Katsumura, A., Sugimura, K., Teramoto, Y., Nishio, Y., 2015. Calcium phosphate mineralization in cellulose derivative/poly (acrylic acid) composites having a chiral nematic mesomorphic structure. *Biomacromolecules* 16, 3959–3969.
- Pella, M.C., Lima-Tenório, M.K., Tenorio-Neto, E.T., Guilherme, M.R., Muniz, E.C., Rubira, A.F., 2018. Chitosan-based hydrogels: from preparation to biomedical applications. *Carbohydr. Polym.* 196, 233–245.

- Reyes-Gasga, J., Martínez-Piñeiro, E.L., Rodríguez-Álvarez, G., Tiznado-Orozco, G.E., García-García, R., Brès, E.F., 2013. XRD and FTIR crystallinity indices in sound human tooth enamel and synthetic hydroxyapatite. *Mater. Sci. Eng., C* 33, 4568–4574.
- Subramanian, R., Sathish, S., Murugan, P., Musthafa, A.M., Elango, M., 2018. Effect of piperine on size, shape and morphology of hydroxyapatite nanoparticles synthesized by the chemical precipitation method. *J. King Saud Uni.-Sci.*
- Sahan, S., Hosseinian, P., Ozdil, D., Turk, M., Aydin, H.M., 2018. Polyurethane-Ceramic matrices as orbital implants. *Int. J. Polymeric Mater. Polymeric Biomater.* 67, 487–493.
- Singh, M.K., Shokuhfar, T., Gracio, J.J.D.A., de Sousa, A.C.M., Ferreira, J.M.D.F., Garmestani, H., Ahzi, S., 2008. Hydroxyapatite modified with carbon-nanotube-reinforced poly (methyl methacrylate): a nanocomposite material for biomedical applications. *Adv. Funct. Mater.* 18, 694–700.
- Surmeneva, M.A., Mukhametkaliyev, T.M., Tyurin, A.I., Teresov, A.D., Koval, N.N., Pirozhkova, T.S., Shuvarin, I.A., Shuklinov, A.V., Zhigachev, A.O., Oehr, C., Surmenev, R.A., 2015. Effect of silicate doping on the structure and mechanical properties of thin nanostructured RF magnetron sputter-deposited hydroxyapatite films. *Surf. Coat. Technol.* 275, 176–184.
- Wang, C., Wang, Y., Meng, H., Wang, X., Zhu, Y., Yu, K., Yuan, X., Wang, A., Guo, Q., Peng, J., Lu, S., 2016. Research progress regarding nanohydroxyapatite and its composite biomaterials in bone defect repair. *Int. J. Polymeric Mater. Polymeric Biomater.* 65, 601–610.
- White, A.A., Best, S.M., Kinloch, I.A., 2007. Hydroxyapatite-carbon nanotube composites for biomedical applications: a review. *Int. J. Appl. Ceram. Technol.* 4, 1–13.
- Zamora-Sequeira, R., Ardao, I., Starbird, R., García-González, C.A., 2018. Conductive nanostructured materials based on poly-(3, 4-ethylenedioxythiophene) (PEDOT) and starch/ $\kappa$ -carrageenan for biomedical applications. *Carbohydr. Polym.* 189, 304–312.
- Zhu, J., Wong, H.M., Yeung, K.W.K., Tjong, S.C., 2011. Spark plasma sintered hydroxyapatite/graphite nanosheet and hydroxyapatite/multiwalled carbon nanotube composites: mechanical and in vitro cellular properties. *Adv. Eng. Mater.* 13, 336–341.
- Zhuo, L., Liao, M., Zheng, L., He, M., Huang, Q., Wei, L., Huang, R., Zhang, S., Lin, X., 2012. Combination therapy with taurine, epigallocatechin gallate and genistein for protection against hepatic fibrosis induced by alcohol in rats. *Biol. Pharm. Bull.* 35, 1802–1810.